# The Effect of Biased Ligand Signaling on Cardiomyocyte Proliferation

by
Syeda Samara Baksh

A thesis submitted to Johns Hopkins University in conformity with the requirements for the degree of Master of Sciences

BIOTECHNOLOGY
Baltimore, MD
August 2016

**Abstract**

Myocardial infarction (MI) (i.e. heart attack) is the permanent death (necrosis) of heart muscle resulting from prolonged lack of oxygen supply (ischemia) (NHLBI, 2015). Without immediate restoration of blood flow, death of heart muscle will ensue (NHLBI, 2015). Every year, more than one million Americans experience MI, and approximately half of them die (Medline Plus, 2015). Though successful return to normal activities post-infarction is highly possible, individuals are nevertheless at risk for complications due to ischemic cardiac tissue (Brown, 2015). The mammalian heart has poor regenerative capabilities – cardiomyocytes cannot proliferate; therefore, cardiac muscle does not repair itself. Recently, the notion that adult cardiomyocytes are unable to proliferate has been challenged (Bergmann, 2009). However, despite intensive research efforts, the mechanisms governing cardiomyocyte cell cycle reentry and proliferation remain unknown. The Dzau lab has recently identified a novel paracrine protein synthesized by mesenchymal stem cells, C3orf58, which they have termed hypoxia and Akt induced stem cell factor (HASF) (Beigi, 2013). Preliminary data has indicated that it harbors the capacity to promote neonatal and adult cardiomyocyte proliferation, and thereby, cardiac regeneration (Beigi, 2013). Previously, I hypothesized that HASF promoted cardiomyocyte proliferation via the CAK complex/ERK signaling pathway (Baksh, 2016). However, I observed that it was IGF-1, not HASF, that promoted cardiomyocyte proliferation via the CAK complex/AKT signaling pathway (Baksh, 2016). Therefore, the goal of this study was to delineate the molecular pathway by which IGF1-AKT-activated CAK complex promotes cardiomyocyte proliferation. IGF1-activated CDKs and cyclins were identified by incubating cells with IGF-1 for 12hr and performing Western blot analysis, probing with cyclin E1 and pCDK2 antibodies. Additionally, the AKT signaling pathway was inhibited by triciribine to

assess to effect of AKT inhibition on CDK2 phosphorylation and cyclin E1 expression. IGF-1 was observed to enhance CDK2 phosphorylation via AKT stimulation and CAK activation. This finding will serve to enhance our understanding of the mechanisms underlying cardiomyocyte cell cycle reentry, and will thus make IGF-1 a potential therapeutic candidate for myocardial repair post-infarction.

*Thesis readers: Dr. Robert Lessick and Dr. Beatrice Kondo*

**Preface**

This dissertation is my original, unpublished, independent work (author S. Baksh).

I would like to thank my PI, Dr. Victor Dzau, for allowing me to complete my thesis research in his lab and funding my project. I am especially grateful to my research mentor, Dr. Conrad Hodgkinson, for his guidance and encouragement during my time at Duke University. I would like to thank Dr. Robert Lessick (thesis advisor and thesis reader) and Dr. Beatrice Kondo (thesis reader) for their guidance and feedback.

**Table of Contents**

**List of Figures**

## Introduction

Myocardial infarction (MI) is the permanent death of heart muscle resulting from prolonged lack of oxygen supply (NHLBI, 2015). The blockage is a result of plaque rupture and subsequent blood clot formation – a coronary artery may become completely blocked if the blood clot grows large enough (NHLBI, 2015). If blood flow is not immediately restored the result is death of heart muscle (NHLBI, 2015). Every year, more than one million Americans experience MI, and approximately half of them die (Medline Plus, 2015). Though countless individuals successfully return to normal activities post-infarction, they are nevertheless at risk for complications due to ischemic cardiac tissue (CDC, 2015). These complications include arrhythmias and heart block, hypotension and congestive heart failure (due to ischemic tissue causing abnormal filling ["diastolic dysfunction"] or abnormal emptying ["systolic dysfunction"]) (Brown, 2015). Several days post-infarction, mechanical complications may arise as a result of "yellow softening" of the myocardial tissue, and pericarditis may ensue as well (Brown, 2015). The mammalian heart has poor regenerative capabilities – unlike other cells, cardiomyocytes are terminally differentiated and possess limited capabilities for cell cycle reentry, and thus, do not undergo division (Kikuchi, 2012). Therefore, cardiac muscle does not have the ability to repair itself, and any damage it sustains is irreversible.

In recent years, the concept of adult cardiomyocytes lacking proliferative abilities has been challenged (Bergmann, 2009), and scientists have been avidly investigating ways to reestablish mitotic activity in cardiomyocytes for myocardial repair and restoration of normal cardiac function post-infarction. Though cardiomyocyte proliferation has been

observed, it is not sufficient for complete myocardial regeneration (Kishore, 2000). Despite the intensive research efforts, the mechanisms underlying cardiomyocyte cell cycle reentry and proliferation remain unclear. However, the Dzau lab has recently identified a novel paracrine protein synthesized by mesenchymal stem cells, C3orf58, and has termed it hypoxia and Akt induced stem cell factor (HASF). They have demonstrated its capacity to promote neonatal and adult cardiomyocyte proliferation, and thereby, cardiac regeneration (Beigi, 2013). Via in vitro studies, Beigi et al. observed that HASF-mediated cardiomyocyte proliferation was dependent upon the stimulation of cyclin-dependent kinase 7 (CDK7).

Among the countless proteins essential to cell cycle control, cyclin-dependent kinases (CDKs) are the most significant. CDKs are small (30 – 40 kD) serine/threonine kinases; they are inactive in the monomeric form, requiring an activating subunit to exert their protein kinase effects (Lodish, 2013; p.884). Though mammalian cells harbor as many as nine CDKs, CDK1, CDK2, CDK4, and CDK6 have been shown to mediate progression of the cell cycle (Lodish, 2013; p.884). By associating with various cyclins, these CDKs regulate the transition of different stages of the cell cycle. CDKs catalyze the phosphorylation of proteins critical to cell cycle progression solely in the presence of cyclins (as indicated by their names) (Nature, 2014). Cyclins themselves harbor no enzymatic activity (Nature, 2014) and have been characterized by three primary features: 1) they associate with and activate CDKs ; 2) they are solely present during the stage of the cell cycle they activate and are absent during the others, and 3) they trigger a series of events to prepare for the approaching cell cycle stage, in addition to regulating their

designated cell cycle stage (Lodish, 2013; p.885). CDK4 and CDK6 are $G_1$ CDKs and bind cyclin D2, promoting entry into the cell cycle; CDK2 is a $G_1$/S phase and S phase CDK and binds cyclins A2 and E1, preparing cells for the S phase; CDK1 is a mitotic CDK and binds cyclins A2 and B1, initiating mitosis (Lodish, 2013; p. 884).

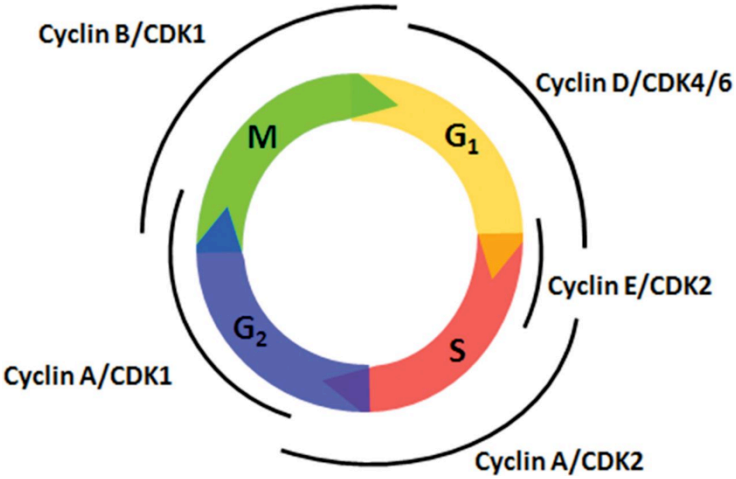


*Image: Suryadinata, 2010.*

CDK7 binds cyclin-H, and additionally, MAT1 (ménage-à-trois 1), a protein that alters the complex's substrate specificity (Patel, 2010) – together, these proteins form the CDK-activating kinase (CAK). CAK is responsible for phosphorylating various CDKs, including CDK1, CDK2, and CDK6 (Lolli, 2005), proteins critical in cell cycle progression, and thereby, cellular proliferation.

HASF activates the Ras–Raf–MEK–ERK (also referred to as MAPK/ERK) signaling pathway (Hodgkinson, C., personal communication, Oct 2015), which regulates diverse biological processes, including cellular proliferation (Liao, 2013). Upon exogenous stimulation, the GTPase Ras is activated (Lodish, 2013; p.739). The protein kinase Raf exists in an inactive state in the unstimulated cell – Ras activation activates Raf kinase activity, and Raf phosphorylates MEK (Lodish, 2013; p.738). MEK subsequently

phosphorylates MAPK/ERK, which translocates to the nucleus and stimulates numerous transcription factors (Lodish, 2013; p.738). These transcription factors promote expression of genes significant to cellular proliferation, including CDKs and cyclins (Chang, 2003).

Insulin-like growth factor 1 (IGF-1) is a hormone found in the blood that mediates the effects of growth hormone (GH) and is essential in early childhood tissue and bone growth (Snyder and Taylor). IGF-1, when bound to its receptor IGF1R, activates the Ras–Raf–MEK–ERK pathway and the PI3K/AKT signaling pathway. The PI3K/AKT pathway, similar to ERK pathway, mediates an array of biological processes, including cellular proliferation (Schiaffino, 2011). Receptor binding results in autophosphorylation of its intrinsic tyrosine kinase, producing docking sites for insulin receptor substrate (IRS), which is subsequently phosphorylated by IGF1R (Schiaffino, 2011). pIRS serves as a docking site for phosphatidylinositol-3-kinase (PI3K); PI3K subsequently phosphorylates membrane phospholipids, producing phosphoinositide-3,4,5-triphosphate (PIP3) from phosphoinositide-4,5-biphosphate (PIP2) (Schiaffino, 2011). PIP3 acts as yet another docking site for phosphoinositide-dependent kinase 1 (PDK1) and Akt (Schiaffino, 2011). PDK1 subsequently phosphorylates Akt at serine 308, resulting in Akt activation (Schiaffino, 2011).

Recently, the Dzau lab has identified a receptor for HASF – IGF1R. Using a yeast two-hybrid screen and co-immunoprecipitation, it was demonstrated that HASF binds IGF1R (Hodgkinson, C., personal communication, Oct 2015). Additionally, the potential of

HASF to stimulate IGF1R and IGF1R-mediated signaling pathways was examined – both HASF and the control, IGF-1, exhibited autophosphorylation of tyrosine-1149 (signifying receptor activation) and promoted ERK phosphorylation (Hodgkinson, C., personal communication, Oct 2015) via the Ras-Raf signaling pathway (Troncoso, 2014). Therefore, it was concluded that HASF activates the Ras-Raf-MEK-ERK pathway.

LL-37 is the cleaved, mature C-terminal peptide of human cathelicidin antimicrobial protein-18 (hCAP-18) and contributes to an array of biological processes such as apoptosis, angiogenesis, and would healing (Girnita, 2012). Like HASF and IGF-1, LL-37 binds to IGF1R; however, it activates only the ERK signaling pathway, not the PI3K/AKT signaling pathway (Girnita, 2012).

The goal of this study is to characterize the molecular mechanisms by which IGF1-AKT-activated CAK complex promotes cardiomyocyte proliferation. Previously, I hypothesized that cardiomyocyte proliferation was mediated by HASF-ERK-CAK. However, I observed that it was IGF1-AKT-CAK that mediates cardiomyocyte proliferation (Baksh, 2016). Therefore, my aim this semester is to further delineate the mechanisms by which IGF1-mediated cardiomyocyte proliferation occurs. To achieve this, the CDKs and cyclins activated by IGF-1 will be identified. Additionally, the effect of CAK knockdown and AKT inhibition on CDK phosphorylation and cyclin expression will be assessed. The results this study will aid in our understanding of the mechanisms governing cardiomyocyte cell cycle reentry and will thus make IGF-1 a potential therapeutic candidate for myocardial repair post-infarction.

## Methods and Materials

siRNA mediated knockdown of the CAK complex

I began with knockdown of *CDK7*and *CCNH*. A day prior to infection, 130,000 H9C2 cells/well were seeded onto T25 flasks. The day the transfection was performed, 10 uM siRNA (6.57 uL) was diluted in optimem-serum-free media (328.75 uL, Optimem-SF, Invitrogen). In a different tube, lipofectamine 2000 (19.72 uL) was added to Optimem-SF (328.75 uL). Solutions were subsequently combined and incubated for 5min at room temperature. 328.75 uL of the transfection complex was added to each flask. Transfection complexes were replaced the next day with fresh growth media (1X DMEM, 10% FBS, 1% Pen/Strep).

Immunoblotting to confirm knockdown of the CAK complex

Three days post-transfection, protein was extracted using 350 ul lysis buffer (1 ml of lysis buffer – 62.5 ul Trizma HCl buffer [1M; pH 7.4], 100 ul 10% SDS, 10 ul protease inhibitors (Roche), 100 ul phosphatase inhibitors (Sigma Aldrich), and 727.5 ul $H_2O$) per well. Protein (20 ug) was denatured by boiling for five minutes and then loaded into wells of a 10-well gel and run for 2h at 120V. Membranes were blocked for one hour in 5% milk (nonfat dry milk [Bio-Rad] in TBST [2.4g Tris, 8g NaCl, 1 ml Tween 20 in 1L water]; pH 7.4 – 7.5) and subsequently probed with B-tubulin (#2146, Cell Signaling Technologies), CDK7 (#2090, Cell Signaling Technologies), or cyclin H (#2927, Cell Signaling Technologies) antibodies at a 1:1000 concentration in 5% milk overnight at 4°C. The following day, membranes were washed 3 times for 5min each in TBST and probed with anti-rabbit secondary antibody (#7074, Cell Signaling Technologies) at a

1:1000 concentration in 5% milk for 75 minutes at room temperature. Membranes were subsequently washed in TBST, placed in ECL for 2min (Amersham ECL Plus™, GE Healthcare; 1:1 ratio of solutions A and B), and visualized via G:BOX Chemi XX6 (Syngene).

To assess proliferation of H9C2s with knockdown of CAK

A day prior to transfection, H9C2s were seeded onto 12-well plates at 20,000 cells/well. The following day, cells underwent *CDK7* and *CCNH* knockdown as described above. Three days post-transfection, cells were serum starved in serum-free media for 6hr and were treated with the following conditions: 1) no treatment; 2) Lipofectamine; 3) siNeg #1; 4) siNeg #2; 5) HASF+CAK knockdown; 6) HASF+siNeg+Lipofectamine 7) IGF-1+CAK knockdown; 8) IGF-1+siNeg+Lipofectamine 9) LL-37+CAK knockdown; and 10) LL-37+siNeg+Lipofectamine. One day post-treatment, proliferation was assessed via BrdU staining – BrdU (0.03 mg/mL) was added to each well and incubated at 37°C for 24h. Following 24h, media was aspirated and cells were fixed in 70% ice-cold ethanol for 5min and subsequently washed in PBS 3 times for 5min each. 1.5 M HCl was then added to the cells for 30m, followed by 2 washes in PBS for 5m each. The cells were subsequently incubated in blocking buffer (0.3% Triton, 5% normal goat serum in PBS) for 1h. Afterwards, anti-BrdU antibody (#5292, Cell Signaling Technologies) was added to the cells at a concentration of 1:500 in antibody dilution buffer (1% BSA in PBS) overnight at 4°C with constant agitation. The next day, cells underwent PBS washes, 3 times for 5min each, and were probed with goat anti-mouse secondary antibody (Alexa Fluor 488 A-11001, ThermoFisher) at a concentration of 1:500 in antibody dilution

buffer for 1hr. During the last PBS wash following secondary incubation, DAPI (1mg/ml) was added to each well. Cells were visualized and were counted with ImageJ.

To assess proliferation of H9C2s with inhibition of the ERK and PI3K/AKT pathways

Cells were trypsinized (0.05% trypsin/EDTA) and seeded onto 12-well plates at 20,000 cells/well. One day post-seeding, cells were serum starved for 6hr and pre-treated with a MEK inhibitor, U0126 (10 uM, Cell Signaling Technologies), and an AKT inhibitor, Triciribine (10 uM, Selleckchem), or vehicle for 2hr prior to the end of serum starvation. Following serum starvation, cells were treated with ligands and their vehicle, sterile/endotoxin-free water (5 ul/ml) or DMSO (1ul/ml), yielding the following conditions: 1) H2O/no treatment; 2) H2O+DMSO; 3) H2O+U0126; 4) H2O+triciribine; 5) HASF; 6) HASF+DMSO; 7) HASF+U0126; 8) HASF+triciribine; 9) IGF-1; 10) IGF-1+DMSO; 11) IGF-1+U0126; 12) IGF-1+triciribine; 13) LL-37; 14) LL-37+DMSO; 15) LL-37+U0126; 16) LL-37+triciribine. Upon 12hr of treatment, cells were stained with BrdU for 24h and assessed for proliferation as described above. Cells were visualized and were counted with ImageJ.

To identify the CDKs and cyclins activated by IGF-1 in cardiomyocytes

Approximately 780,000 H9C2 cells were seeded into T150 flasks; upon 50 – 70% confluence, cells were serum starved in serum-free media (1X DMEM, 1% Pen/Strep) for 6hr and treated with IGF-1 (1 uL/mL) for 12h. Upon ~80% confluency, at which point the cells were in a linear growth phase, protein was extracted using 500 uL lysis buffer. Following boiling for five minutes, 40 ug of protein was loaded into wells of a 10-well

gel and run for 2hr at 120V. Membranes were blocked for one hour in 5% milk (nonfat dry milk [Bio-Rad] in TBST [2.4g Tris, 8g NaCl, 1 ml Tween 20 in 1L water]; pH 7.4 – 7.5) and subsequently probed with pCDK2 (#2561, Cell Signaling Technologies), cyclin A2 (#4656, Cell Signaling Technologies), cyclin B1 (#4138, Cell Signaling Technologies), cyclin E1 (#4129, Cell Signaling Technologies), and B-tubulin (#2146, Cell Signaling Technologies), at a 1:1000 concentration in 5% BSA overnight at 4°C with constant agitation. The following day, membranes were washed 3 times with TBST for 5min each and probed with anti-rabbit secondary antibody (#7074, Cell Signaling Technologies) at a 1:1000 concentration in 5% BSA for 75m at room temperature. Membranes were subsequently washed in TBST, placed in ECL for 2min (Amersham ECL Plus™, GE Healthcare; 1:1 ratio of solutions A and B), and visualized via G:BOX Chemi XX6 (Syngene).

To determine the effect of CAK knockdown on IGF1-mediated activation of CDKs and cyclins.

A day prior to infection, 780,000 H9C2 cells were seeded into T150 flasks. The day the transfection was performed, 10 uM siRNA (39.48 uL) was diluted in optimem-serum-free media (1,972.5 uL, Optimem-SF, Invitrogen). In a different tube, lipofectamine 2000 (118.38 uL) was added to Optimem-SF (1,972.5 uL). Solutions were subsequently combined and incubated for 5m at room temperature. 1,972.5 uL of the transfection complex was added to each flask. Media was changed the following day to standard growth media (1X DMEM, 10% FBS, 1% Pen/Strep). Three days post-transfection, cells were serum starved and treated with IGF-1 as described above. Western blot was used to evaluate protein expression as described above.

To determine the effect of AKT inhibition on IGF1-mediated activation of CDKs and cyclins.

Cells were seeded and serum starved as described above and pre-treated with the AKT inhibitor triciribine (10 uM, Selleckchem) 2h prior to the end of serum starvation. Following serum starvation, cells were treated with ligands as described above. Afterwards, protein was extracted and Western blot analysis was performed.

To validate CAK-mediated phosphorylation of CDKs and activation of cyclins.

*DpnI Cloning*

Initially, a CDK7 plasmid was purchased (#MR205228, Origene), and mutant primers were designed complementary to the CDK7 binding site (position 41; a lysine was converted to an alanine to induce a dominant negative mutation) and active site (position 137; an alanine was converted to an aspartate to induce a constitutively active mutation) (Eurofins).

| Primer | Sequence |
|---|---|
| Mutant Primer 41F | CGTCGCTATTCGCAAAATCAA |
| Mutant Primer 41R | TTGATTTTCGCAATAGCGACG |
| Mutant Primer 137F | CACAGGGCTCTGAAACCAA |
| Mutant Primer 137R | TTGGTTTCAGAGCCCTGTG |

Afterwards, site-directed mutagenesis was performed via PCR (5331 Mastercycler Gradient, Eppendorf) using Phusion® High-Fidelity DNA Polymerase (#M0530, New England Biolabs). Three reactions were run –

- one containing muPrimer-41: 41F + 41R
- one containing muPrimer-137: 137F + 137R
- one a control, containing muPrimer-41: 41F + 41R with no enzyme.

One 50 uL reaction contained the following reagents:

| **Reagent** | **50 µl Reaction** | **Final Concentration** |
|---|---|---|
| 5X Phusion HF Buffer | 10 µl | 1X |
| 10 mM dNTPs | 1 µl | 200 µM |
| 10 µM Forward Primer | 2.5 µl | 0.5 µM |
| 10 µM Reverse Primer | 2.5 µl | 0.5 µM |
| DMSO | 1.5 µl | 3% |
| Phusion DNA Polymerase | 0.5 µl | 1.0 units/50 µl PCR |
| Template DNA | 1 µl | 10 ng |
| Nuclease-free water | Up to 50 ul | |

Thermocycling conditions for PCR were as follows:

| **STEP** | **TEMP** | **TIME** |
|---|---|---|
| Initial Denaturation | 98°C | 30 seconds |
| 30 Cycles | 98°C<br>58°C<br>72°C | 10 seconds<br>30 seconds<br>30 seconds |
| Final Extension | 72°C | 10 minutes |
| Hold | 4°C | |

Following PCR, the PCR product underwent purification using QIAquick PCR Purification Kit (#28106, Qiagen). Purification was performed as per manufacturer's

protocol and DNA eluted into 50ul of buffer EB (10mM Tris pH7.5). Afterwards, 10 uL of purified DNA was mixed with 1.67 uL 5X Nucleic Acid Sample Loading Buffer (#1610767, Bio-Rad) and loaded into wells of a 0.8% agarose gel (100 mL 1X TAE buffer, 0.8 g agarose, and 10 uL Green Gene Safe DNA dye [#RE0500, Southern Biolabs]). The gel was run at 120 V for 90m and visualized under UV. The following day, the PCR product underwent DpnI digestion – 26 uL of PCR product was digested in 3 uL CutSmart® Buffer (#B7204S, New England Biosciences) and 1 uL DpnI (#R0176, New England Biosciences) for 150m in a 37°C water bath. Next, bacterial transformation was performed using MAX Efficiency® DH5α™ Competent Cells (#18258012, ThermoFisher) per manufacturer's instructions. 100 uL of competent cells was plated onto LB agar plates, which contained Kanamycin (50 ug/mL final concentration). Plates were placed in a 37°C incubator over-night and checked for colonies the next day.

To troubleshoot the PCR, three separate PCRs were run, each containing the three aforementioned reactions (control, 41, and 137), with three different thermocycling conditions. The first PCR was run with an annealing temperature of 61°C, the second PCR was run with a denaturation time of 30sec, and the third PCR was run with an extension time of 270sec. For all three PCRs, the cycle number was increased to 35. Subsequently, PCR products were run on agarose gels, purified, digested, transformed, and plated onto agar plates with the addition of kanamycin as described above. Additionally, parental plasmid DNA was diluted 1:100, transformed, and plated to serve as a control.

*Mutagenic PCR*

Mutagenic PCR was performed in a two-step reaction. The first step was to carry out the following four reactions:

| |
|---|
| 41 F mutant primer + VP 1.5 (5') sequencing primer |
| 41 R mutant primer + XL39 (3') sequencing primer |
| 137 F mutant primer + VP 1.5 (5') sequencing primer |
| 137 R mutant primer + XL39 (3') sequencing primer |

Thermocycling conditions for PCR were as follows:

| **STEP** | **TEMP** | **TIME** |
|---|---|---|
| Initial Denaturation | 98°C | 30 seconds |
| 35 Cycles | 98°C<br>50°C<br>72°C | 10 seconds<br>30 seconds<br>5 minutes |
| Final Extension | 72°C | 10 minutes |
| Hold | 4°C | |

Sequencing primers were added during the last minute of the third PCR cycle. PCR products were run on agarose gels and purified as described above.

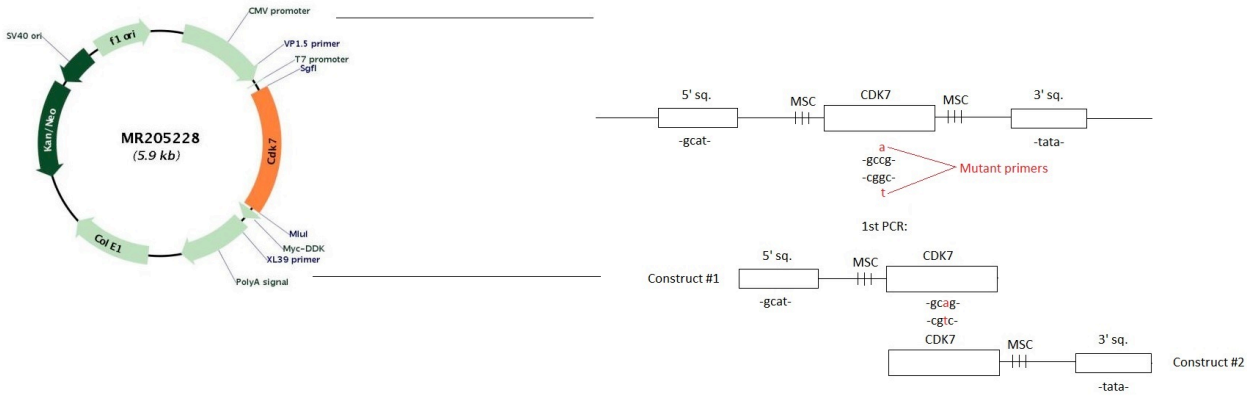


Afterwards, a second PCR was run containing three reactions – 41F3' + 41R5', 137F3' + 137R5', and a control containing solely 41F3'. VP 1.5 and XL39 were added during the last minute of the third PCR cycle. Subsequently, PCR products were run on an agarose gel and visualized as described above.

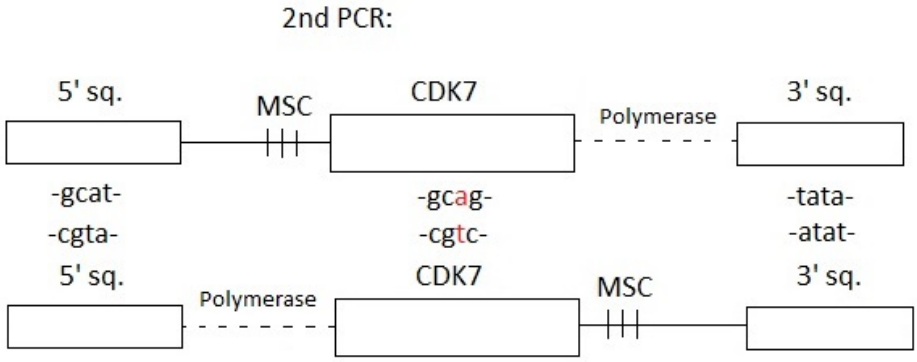


To prevent parental plasmid contamination of PCR products, PCR was repeated as previously mentioned [(41 F mutant primer + VP 1.5 (5') sequencing primer; 41 R mutant primer + XL39 (3') sequencing primer; 137 F mutant primer + VP 1.5 (5'); 137 R mutant primer + XL39 (3')], and bands were gel purified using the QIAquick® Gel Extraction Kit (#28704, Qiagen). Subsequently, the concentration of gel purified DNA was measured via NanoDrop™ 2000 –

| **Construct** | **Concentration (ng/uL)** | **260/280** |
|---|---|---|
| 41F3’ | 26.3 | 1.93 |
| 41R5’ | 10 | 1.88 |
| 137F3’ | 37 | 1.90 |
| 137R5’ | 28.2 | 1.83 |

A second PCR containing seven reactions was run – H2O control, 41F3’, 41R5’, 41F3’+41R5’, 137F3’, 137R5’, and 137F3’+137R5’ – and cycle number was decreased to 25. PCR products were subsequently run on an agarose gel and visualized.

To further optimize the PCR, gel purified DNA was run on an agarose gel at approximately equal molarities with double the concentration of Mg++ (from 1.5 mM to 3 mM) and no more than 10 ng of DNA per well. The following are example calculations:

Assuming 1 bp is 121 g/mol, 1.5 kb (size of construct) = 181,500 g/mol.

<u>41F3’ construct</u> –

26.3 ng/uL = $2.63 \times 10^{-8}$ g/uL

$2.63 \times 10^{-8}$ g / $1 \times 10^{-6}$ L = 0.0263 g/L

Molarity = 0.0263 g/L / 181,500 g/mol

= $1.45 \times 10^{-7}$ mols/L = **145 nM**

41R5' construct –

10 ng/uL = 1 x $10^{-8}$ g/uL

1 x $10^{-8}$ g / 1 x $10^{-6}$ L = 0.01 g/L

Molarity = 0.01 g/L / 181,500 g/mol

= 5.51 x $10^{-8}$ mol/L

= **55.1 nM**

41F3' : 41R5'

1 : 3 = 4

10 ng (total amount of DNA per reaction) / 4 = 2.5

1 x 2.5 = 2.5 ng

3 x 2.5 = 7.5 ng

2.5 ng : 7.5 ng per reaction.

## Results

The goal of this study was to delineate the molecular mechanisms by which IGF1-AKT-activated CAK complex promotes cardiomyocyte proliferation. Last semester, I observed that cardiomyocyte proliferation is mediated by IGF1-AKT-CAK. Therefore, my aim this semester was to further characterize the mechanisms by which IGF1-mediated cardiomyocyte proliferation occurs. To achieve this, the CDKs and cyclins activated by IGF-1 were identified and the effect of CAK knockdown and AKT inhibition on CDK phosphorylation and cyclin expression was evaluated.

IGF-1 promotes cardiomyocyte proliferation via the CAK complex

I began by validating my finding from last semester in which it was observed that IGF-1 promotes cardiomyocyte proliferation via the CAK complex. Upon knocking down *CDK7* and *CCNH*, knockdown was confirmed via Western blot analysis.

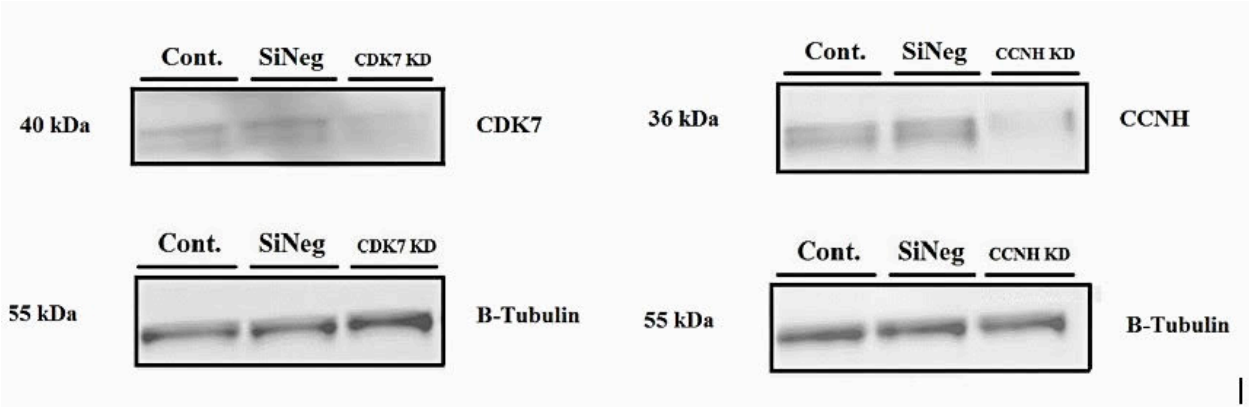


**Figure 1.** Western blot analysis for CDK7 and cyclin H upon knockdown; B-tubulin was used as the loading control. $n = 2$

Following confirmation of knockdown, a proliferation assay was performed to validate the role of the CAK complex in IGF-1-mediated cardiomyocyte proliferation, as demonstrated last semester (**Figure 2.,** compare bars "IGF-1 (CAK Knockdown)" [mean = 47.68%] and "IGF-1+siNeg+Lipofectamine" [mean = 62.73%] along with the

remainder of the controls [H2O/no treatment, mean = 59.3%; lipofectamine, mean = 57.86%; siRNA negative control #1, mean = 58.22%; siRNA negative control #2, mean = 53.57%; HASF (CAK knockdown), mean = 63.72%; HASF+siNeg+Lipofectamine, mean = 68.49%; LL-37 (CAK knockdown), mean = 61.09%; LL-37+siNeg+Lipofectamine, mean = 67.36%]) and **Figure 3**., compare images 7 and 8, along with the remainder of the controls [images 1 – 6; 9 - 10]). Significance was found between CAK knockdown H9C2s treated with IGF-1 and H9C2s containing a functional CAK complex treated with IGF-1, siRNA negative control, and Lipofectamine (p-value: 0.0285).

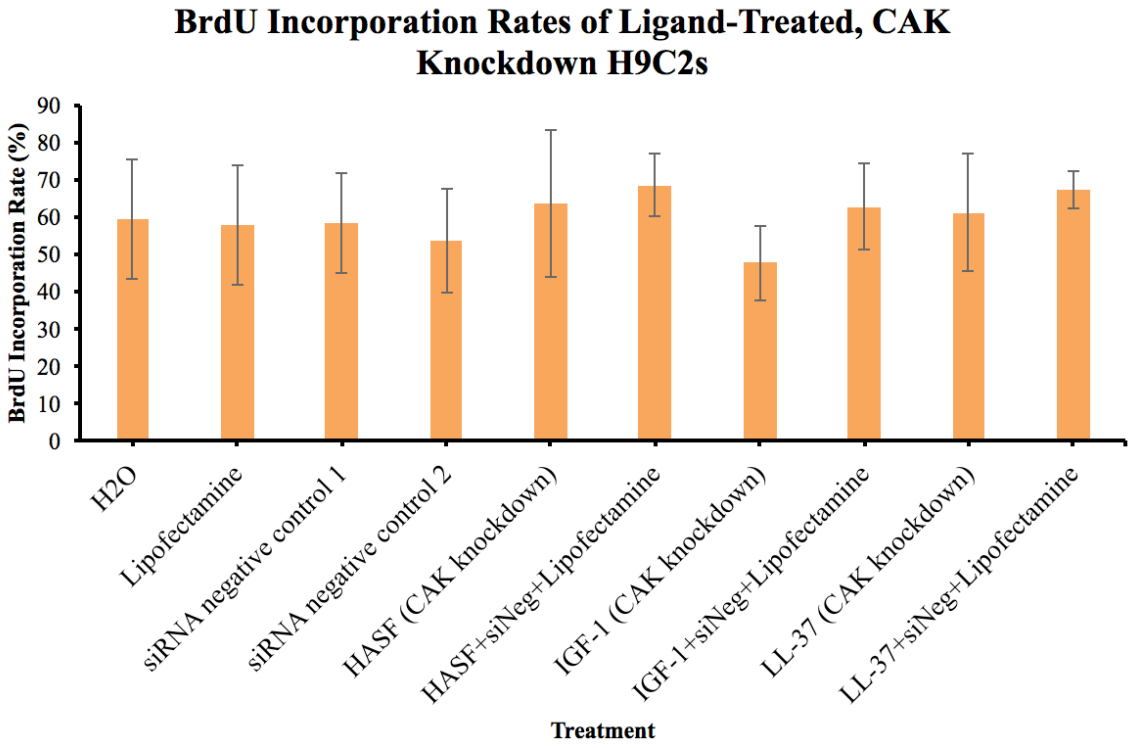


**Figure 2.** BrdU incorporation rates of CAK knockdown H9C2s induced with HASF, IGF-1, and LL-37; $n = 3$

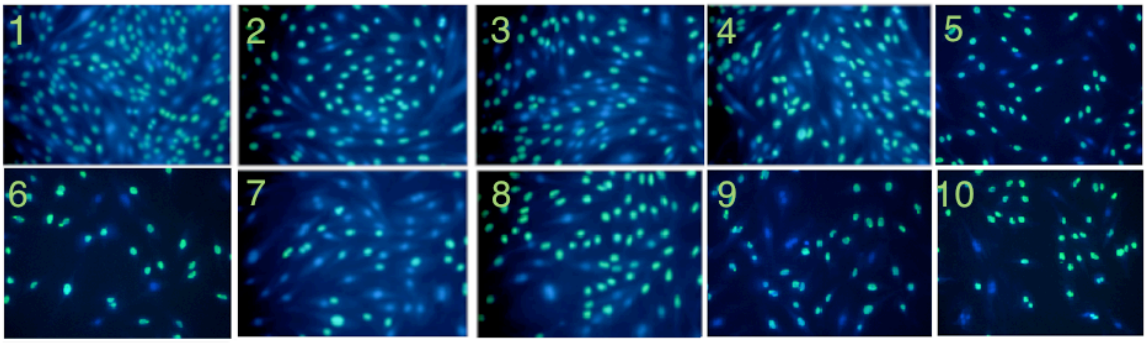


**Figure 3.** Immunohistochemical analysis of CAK knockdown H9C2s induced with HASF, IGF-1, and LL-37. BrdU staining was utilized to assess rates of incorporation in cells containing and lacking functional CAK complexes. Left to right, top to bottom:1) no treatment; 2) Lipofectamine; 3) siNeg #1; 4) siNeg #2; 5) HASF (CAK knockdown); 6) HASF+siNeg+Lipofectamine; 7) IGF-1 (CAK knockdown); 8) IGF-1+siNeg+Lipofectamine; 9) LL-37 (CAK knockdown); 10) LL-37+siNeg+Lipofectamine; $n = 3$

IGF-1 reduces H9C2 proliferation via the AKT signaling pathway

Next, I validated the finding from last semester in which it was observed that AKT inhibition reduces H9C2 proliferation. Cells were incubated with the pERK inhibitor, U0126, and the AKT inhibitor, triciribine. HASF, IGF-1, and LL37 were used to enhance cardiomyocyte proliferation. As demonstrated in **Figure 4.,** treatment with ligands caused cells to exhibit average BrdU incorporation rates of 87.14%, 81.80%, and 87.1% for HASF, IGF-1, and LL-37, respectively, compared to the control, 78.87%. However, when treated with triciribine (**Figure 5.**), the average BrdU incorporation rates for H9C2s induced with HASF, IGF-1, and LL-37 are 65.15%, 71.74%, and 85.02%, respectively. When treated with U0126, the average BrdU incorporation rates of H9C2s induced with HASF, IGF-1, and LL-37 are 72.61%, 81.53%, and 81.55%, respectively. Significance was found between H9C2s treated with IGF-1 and H9C2s treated with IGF-1+triciribine (p-value: 0.03705).

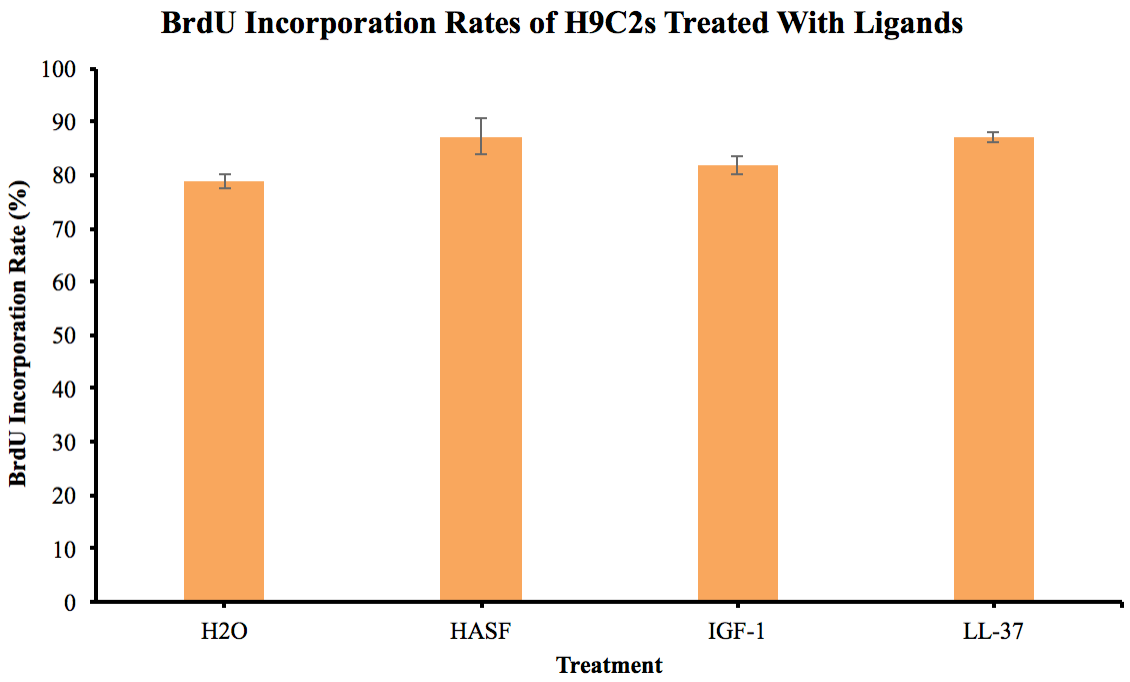


**Figure 4.** BrdU incorporation rates of H9C2s induced with HASF, IGF-1, and LL-37; *n* = 3.

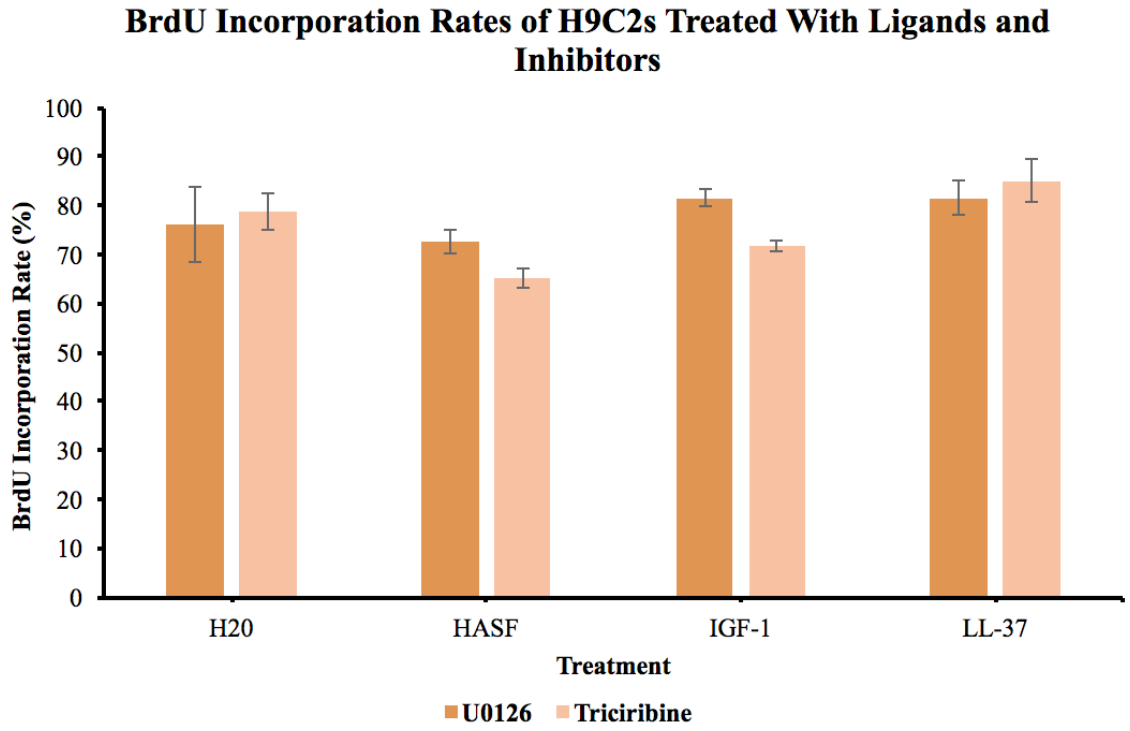


**Figure 5.** BrdU incorporation rates of ligand-induced H9C2s treated with U0126 and triciribine; *n* = 3.

IGF-1 enhances phosphorylation of CDK2, but does not enhance cyclin E1 expression

Western blot analysis was utilized to evaluate the cyclins activated by IGF-1. Blots were probed with cyclin A2, cyclin B1, and cyclin E1 antibodies, however, only the cyclin E1 bands were noticeably visible. As demonstrated in **Figure 6,** (compare left band and bar, respectively, "H2O (Cont.)" with right band and bar, respectively, "IGF-1")**,** IGF-1 did not enhance cyclin E1 expression.

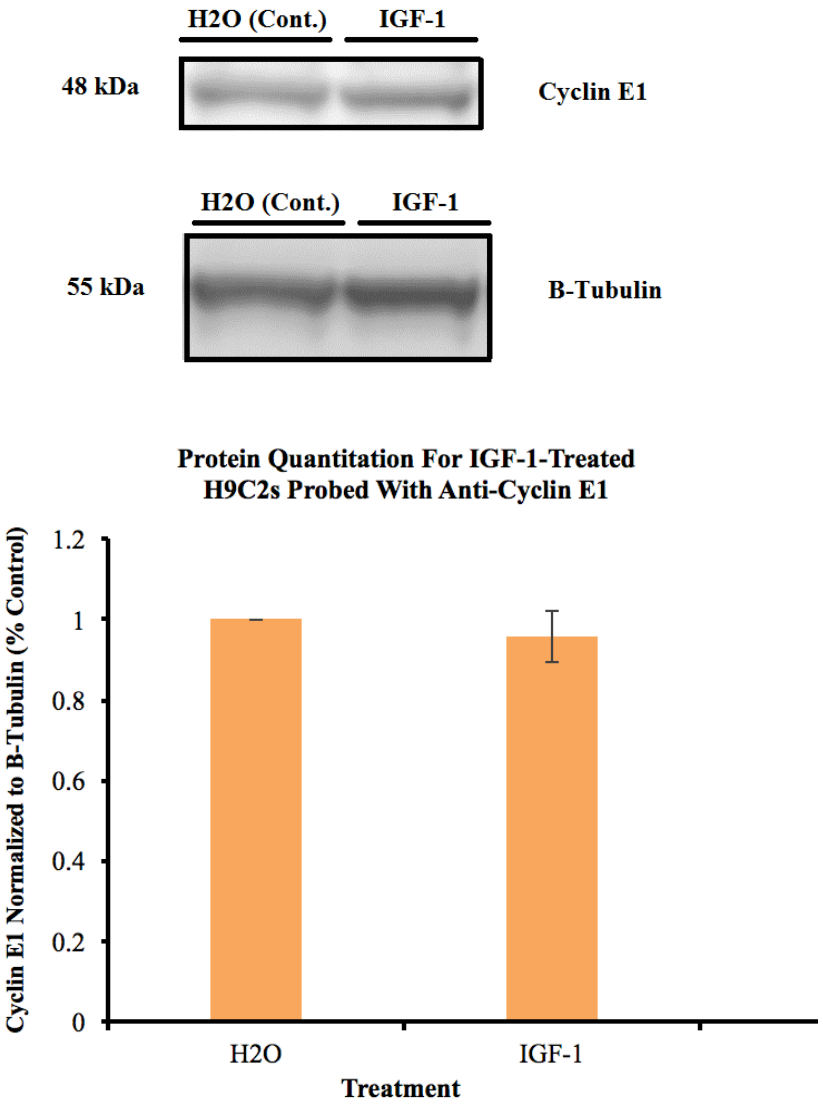


**Figure 6.** Western blot analysis and protein quantitation for H9C2s treated with IGF-1 and probed with anti-cyclin E1; B-tubulin was used as the loading control; $n = 3$.

Blots were then probed with pCDK2. As demonstrated in **Figure 7,** (compare left band and bar, respectively, "H2O (Cont.)" with right band and bar, respectively, "IGF-1"), IGF-1 enhanced phosphorylation of CDK2 by ~30%.

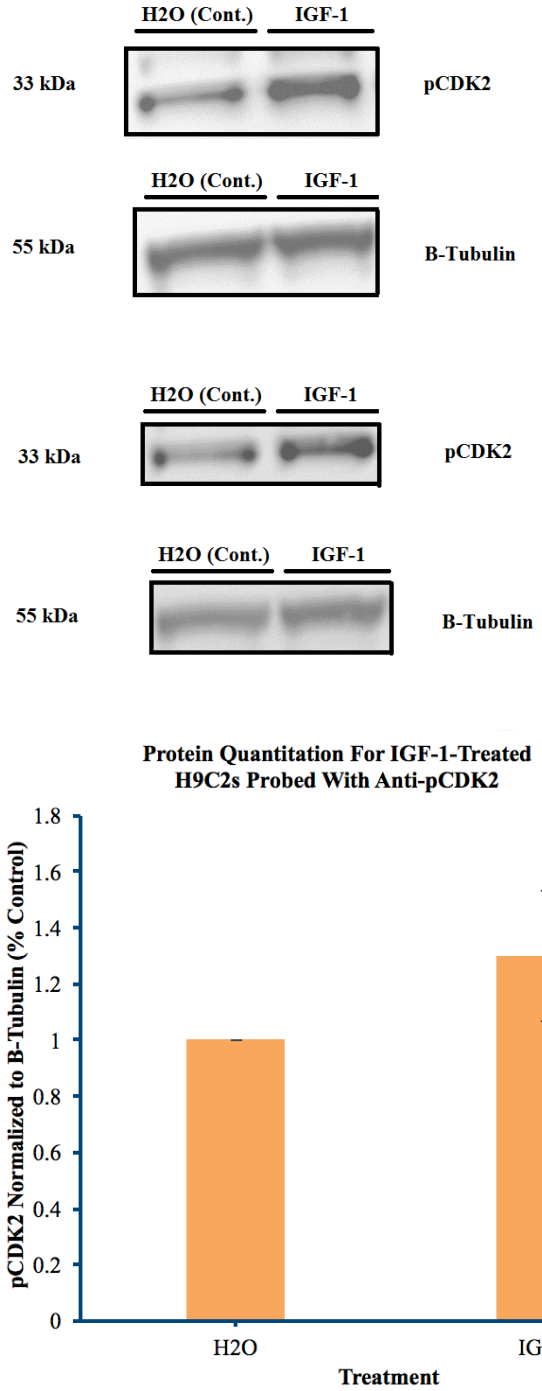


**Figure 7.** Western blot analysis and protein quantitation for H9C2s treated with IGF-1 and probed with anti-pCDK2; B-tubulin was used as the loading control; $n = 3$.

CAK Knockdown Resulted in Uninterpretable Data

The effect of CAK knockdown on cyclin E1 expression and phosphorylation of CDK2 was evaluated via Western blot analysis. Unfortunately, both the siRNA negative control and the transfection reagent lipofectamine impacted cyclin E1 expression and CDK2 phosphorylation (**Figure 8,** compare left band and bar "no treatment," center band and bar "si(-)," and right band and bar "lipofectamine"). Thus, it was difficult to determine if IGF-1 modified cyclin E1 expression and CDK2 phosphorylation in the absence of the CAK complex in H9C2s induced with IGF-1 (not shown).

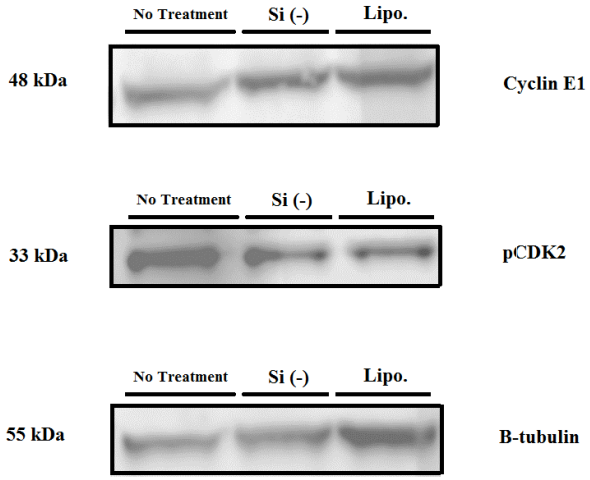

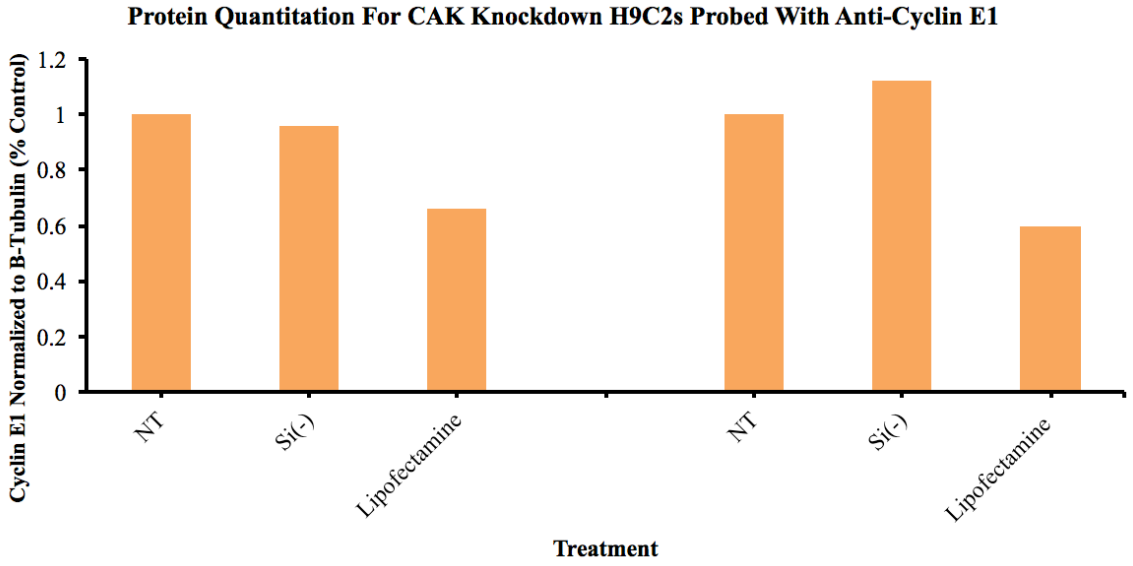


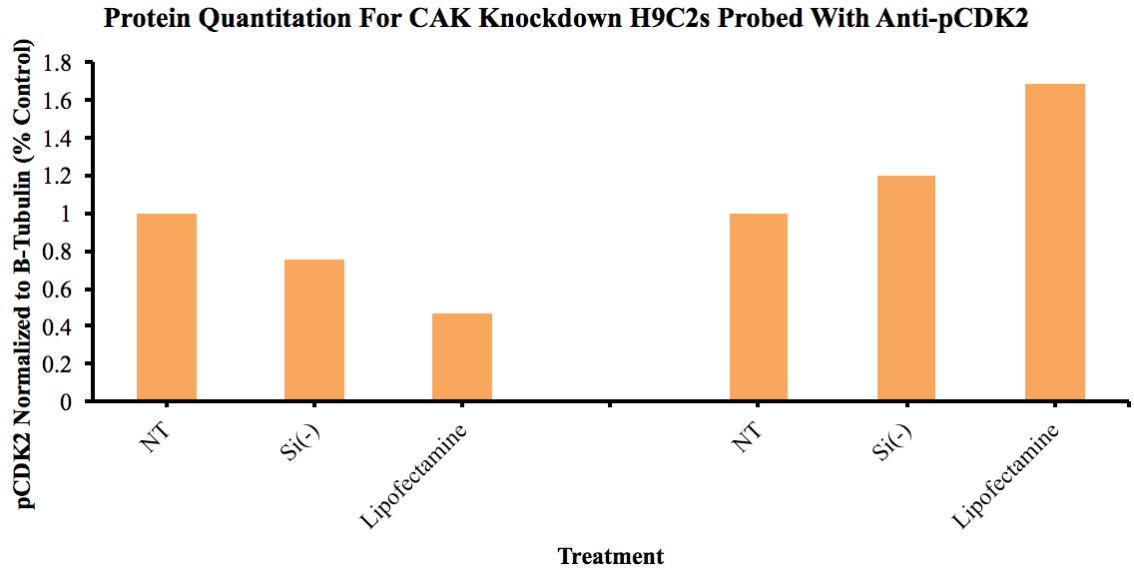


**Figure 8.** Western blot analysis and protein quantitation for H9C2s treated with transfection reagents and probed with anti-cyclin E1 and –pCDK2. CAK knockdown H9C2s induced with IGF-1 not shown due to lack of interpretability; $n = 2$.

AKT inhibits phosphorylation of IGF-1-activated CDK2, but does not inhibit cyclin E1 expression.

Western blot analysis was utilized to assess the effect of AKT inhibition on cyclin E1 expression and CDK2 phosphorylation. Cells were incubated with the AKT inhibitor,

triciribine (Tri). This AKT pharmacological inhibitor had no effect on cyclin E1 expression following IGF-1 treatment (**Figure 9.,** compare left band and bar, "H2O (Cont.)" center band and bar, "(IGF-1)" and right band and bar, "IGF-1+Tri.,").

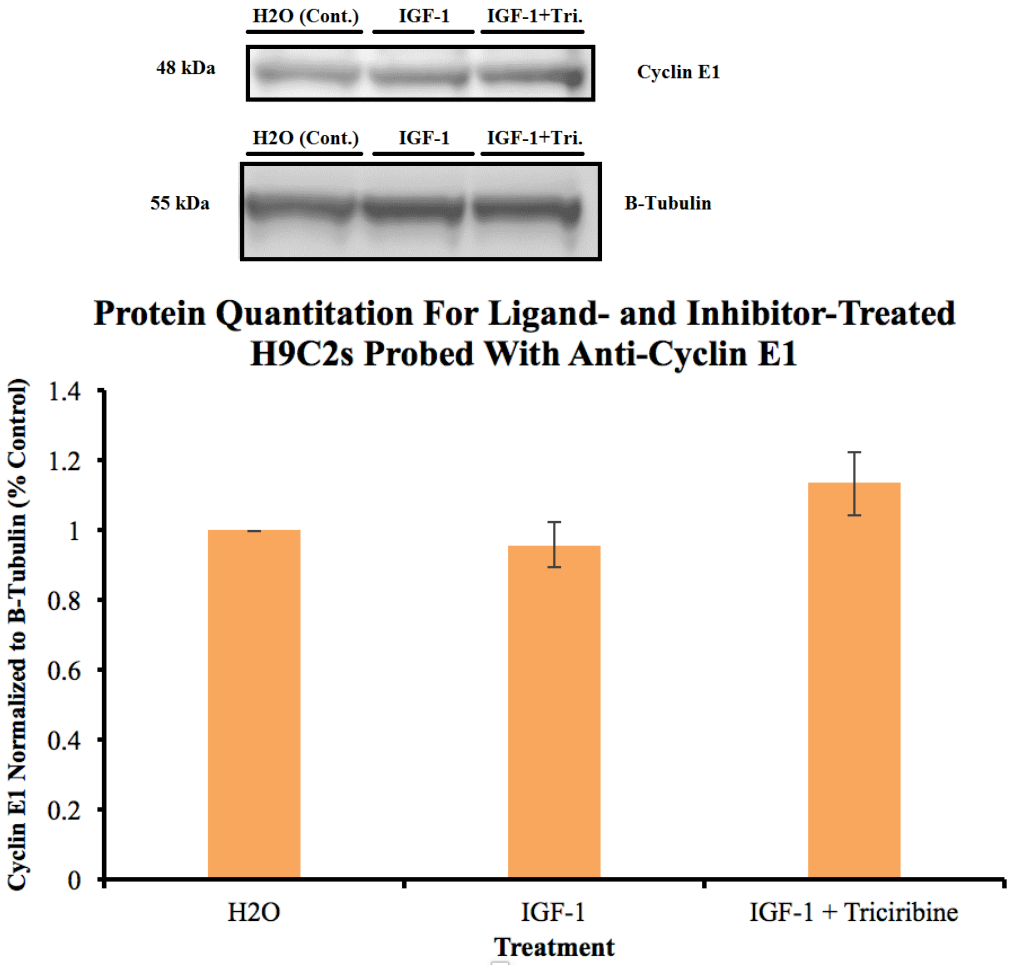


**Figure 9.** Western blot analysis and protein quantitation for IGF-1-induced H9C2s treated with triciribine and probed with anti-cyclin E1; B-tubulin was used as the loading control; $n = 3$.

In contrast, triciribine markedly inhibited IGF-1 mediated phosphorylation of CDK2 (**Figure 10.,** compare left band and bar, "H2O (Cont.)" center band and bar, "(IGF-1)" and right band and bar, "IGF-1+Tri.), reducing phosphorylation to baseline levels.

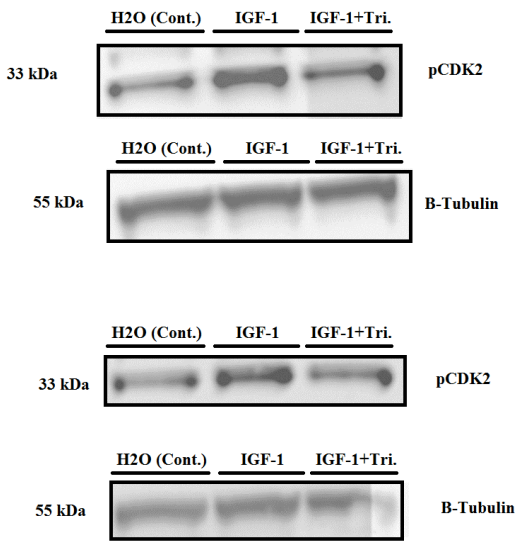


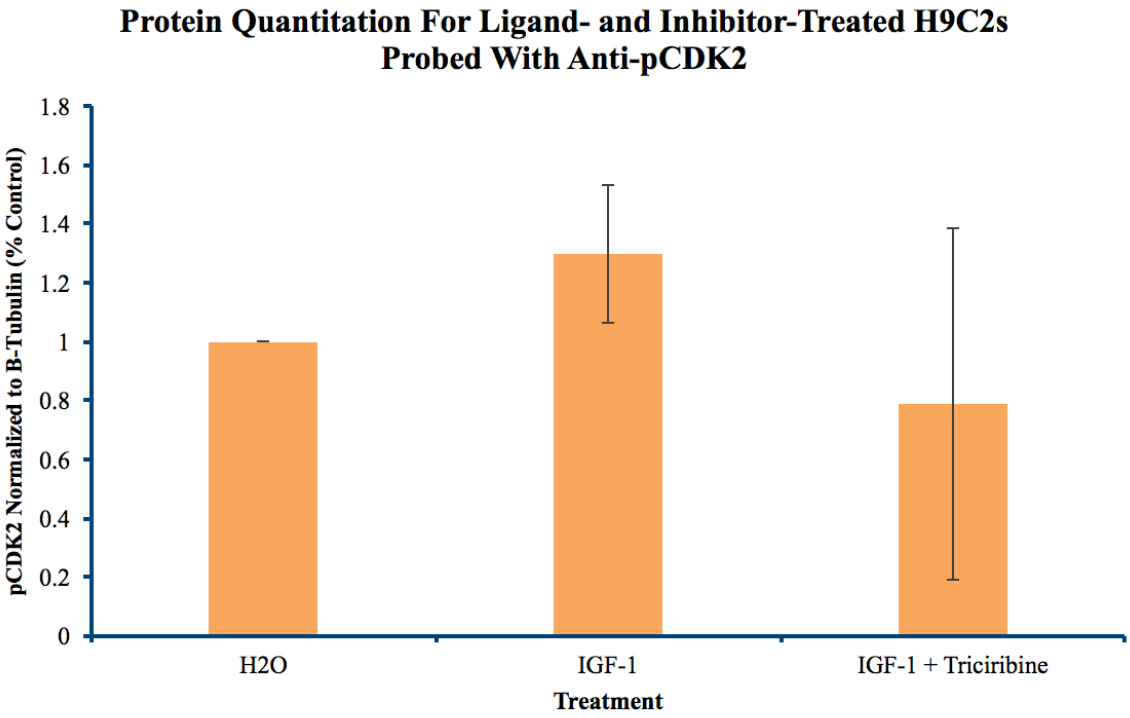


**Figure 10.** Western blot analysis and protein quantitation for IGF-1-induced H9C2s treated with triciribine and probed with anti- pCDK2; B-tubulin was used as the loading control; $n = 3$.

Designing mutant CDK7 variants to validate the role of CAK in IGF-1 mediated proliferation.

To validate CAK-mediated phosphorylation of CDKs and activation of cyclins, transfection of groups of cardiomyocytes with a dominant negative form of CAK and a constitutively active form of CAK would have been performed. IGF-1 would have been added to the wells of a 12-well plate to stimulate proliferation. Following transfection, Western blot analysis would have been performed to detect CDKs and cyclins. Afterwards, BrdU proliferation assays would have been performed as a final readout.

In order to create dominant negative and constitutively active CDK7 constructs for transfection into H9C2s, site-directed mutagenesis via DpnI cloning was first employed. Despite several attempts where annealing temperature, denaturation, and elongation times were altered, as well as cycle number, no bacterial colonies were observed. This was not due to bacterial transformation as the positive control DNA yielded colonies.

As DpnI cloning was not working as intended, an alternative two-step strategy was utilized. In the first step, PCR was performed using sequencing primers VP 1.5 (5') and XL39 (3') and mutant primers to produce four individual constructs – 41F3', 41R5', 137F3', 137R5' (**Figure 11**). In the second step, respective constructs were combined (i.e. 41F3'+41R5' and 137F3'+137R5'), and after three rounds without primers to allow the polymerase to fill-in the overhangs, the DNA was amplified with the sequencing primers, and subsequently run on an agarose gel. As depicted in **Figure 12,** the control lane (41F3') contains a band at 1500 bp, indicative of parental plasmid contamination.

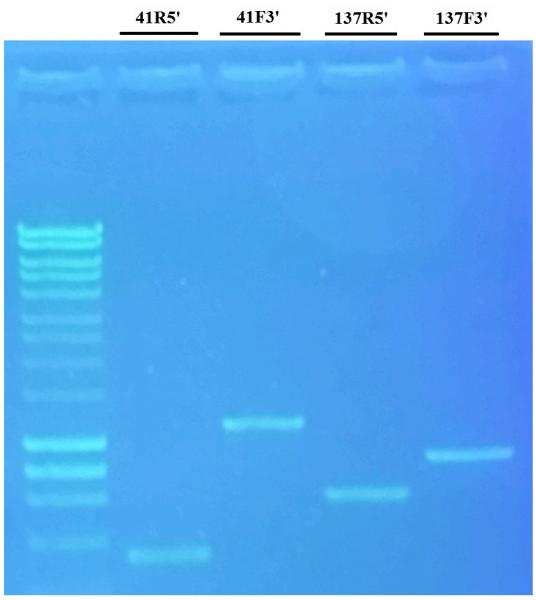


**Figure 11.** Gel electrophoresis for individual constructs 41R5', 41F3', 137R5', and 137F3' amplified via PCR.

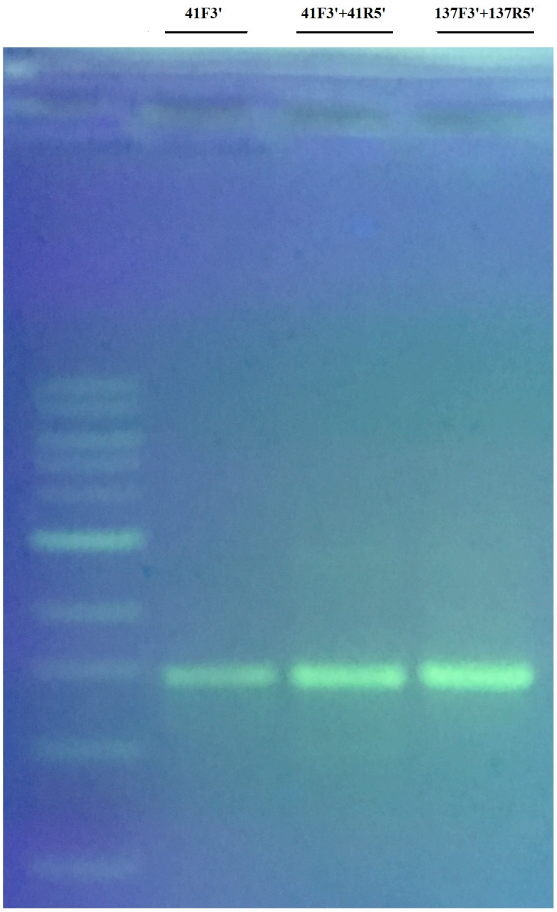


**Figure 12.** Gel electrophoresis for combined constructs 41F3'+41R5' and 137F3'+137R5' in addition to control 41F3'. Presence of band in control lane is suggestive of parental plasmid contamination.

To prevent parental plasmid contamination, 41F3', 41R5', 137F3', and 137R5' bands were gel purified, and purified DNA was amplified as described above. PCR products were then visualized (**Figure. 13**).

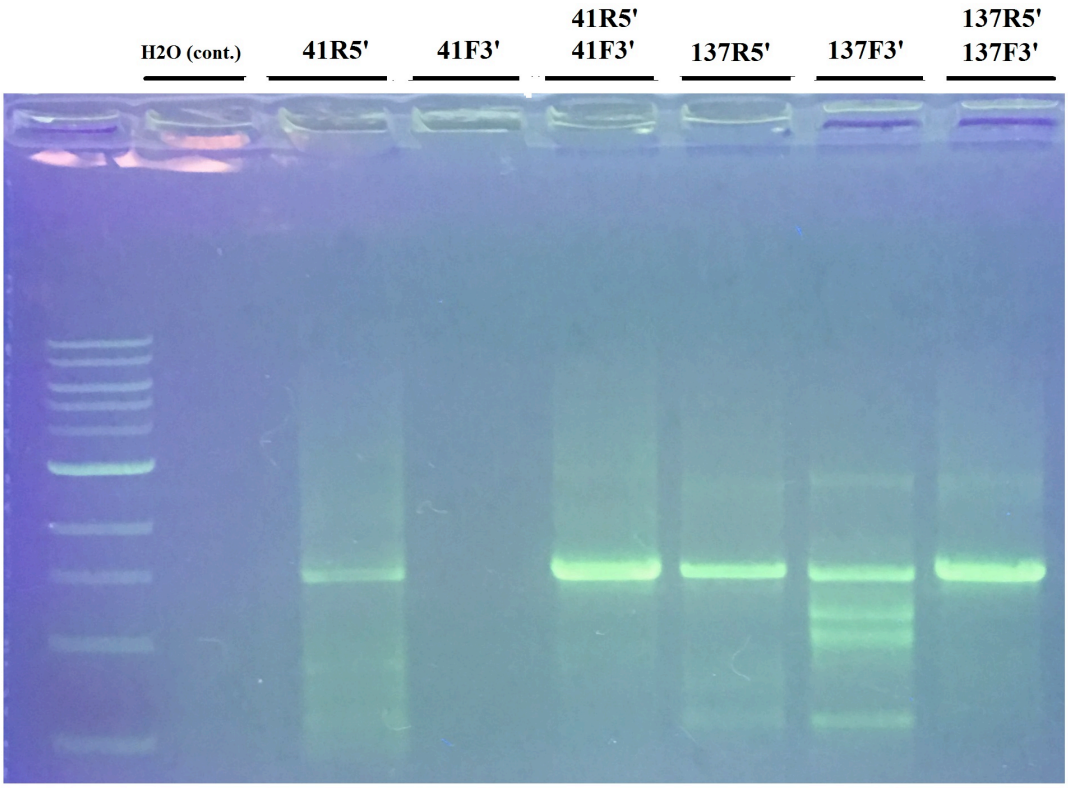


**Figure 13.** Gel electrophoresis for combined constructs 41R5'+41F3' and 137R5'+137F3' in addition to controls H2O, 41R5', 41F3', 137R5', and 137F3'. Presence of bands in 41R5', 137R5', and 137F3' lanes indicates plasmid contamination.

Plasmid contamination persisted (bands present in 41R5', 137R5', and 137F3' lanes), and therefore further optimization was necessary. Three alternatives were attempted:

1) PCR cycle number reduced from 35 to 25

2) PCR performed with respective constructs at approximately equal molarities and no more than 10 ng DNA per lane (**Figure 14**), and finally,

3) PCR performed with double Mg++ concentration (**Figure 15**).

Plasmid contamination was the least in PCR #3 (**Figure 15**), as demonstrated by the lack of bands in the 41R5’ and 41F3’ lanes and the presence of faint bands in the 137R5’ and 137F3’ lanes.

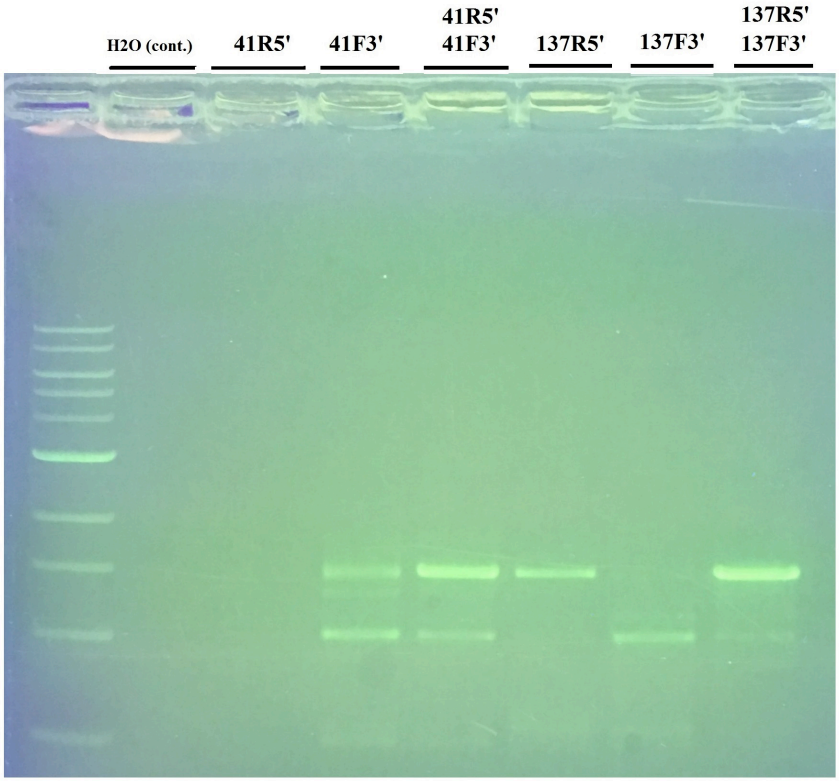


**Figure 14.** Gel electrophoresis for combined constructs 41R5’+41F3’ and 137R5’+137F3’ in addition to controls H2O, 41R5’, 41F3’, 137R5’, and 137F3’. Respective constructs at approximately equal molarities and no more than 10 ng DNA per lane in addition to PCR cycle number 25.

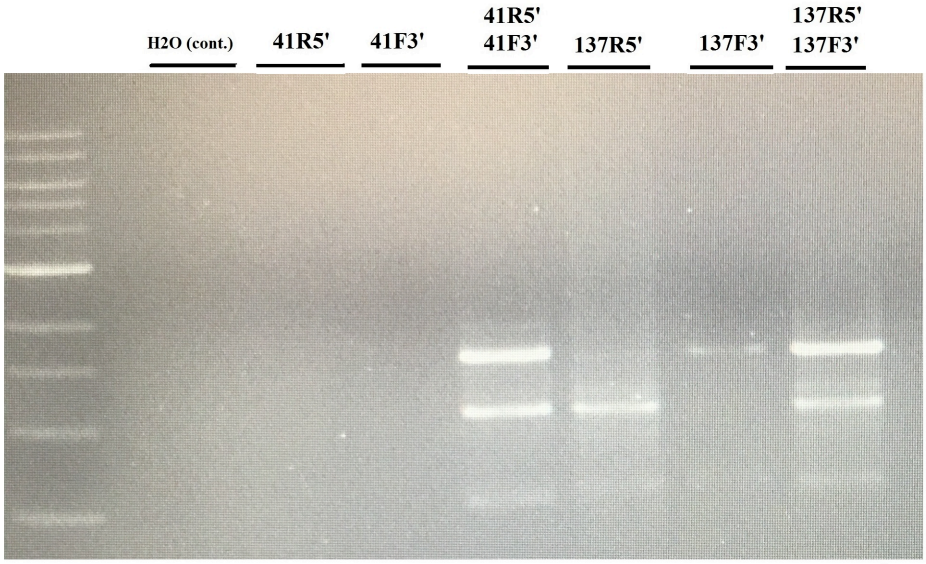


**Figure 15.** Gel electrophoresis for combined constructs 41R5'+41F3' and 137R5'+137F3' in addition to controls H2O, 41R5', 41F3', 137R5', and 137F3'. Mg++ concentration doubled (from 1.5 mM to 3 mM). Respective constructs at approximately equal molarities and no more than 10 ng DNA per lane in addition to PCR cycle number 25.

## Discussion

*The role of CAK and AKT in stimulated cardiomyocyte proliferation.*

The Dzau lab has previously demonstrated that the novel paracrine protein HASF promotes neonatal and adult cardiomyocyte proliferation. During semester one, I initially hypothesized that HASF mediated cardiomyocyte proliferation via the CAK complex. CAK knockdown data, however, did not support that hypothesis – when performing BrdU staining for cell proliferation, I expected to see decreased proliferation in CAK knockdown cells induced with HASF. Instead, I observed decreased proliferation only in cells induced with IGF-1. This, along with the significance found between CAK knockdown H9C2s treated with IGF-1 and H9C2s containing a functional CAK complex treated with IGF-1, siRNA negative control, and Lipofectamine (p-value: 0.0285), indicated that IGF-1 promotes cardiomyocyte proliferation via the CAK complex and HASF does not, suggesting that the CAK complex is AKT-dependent.

The data represented in Figure 5 validated the importance of AKT in IGF1-mediated cardiomyocyte proliferation, as the AKT inhibitor triciribine reduced the proliferative effect of IGF-1 (significance between H9C2s treated with IGF-1 and H9C2s treated with IGF-1+triciribine – p-value: 0.03705), but the pERK inhibitor, U0126, did not.

*The role of IGF-1, AKT, and CAK in the cardiomyocyte cell cycle.*

To identify the CDKs and cyclins activated by IGF-1 in cardiomyocytes, I initially probed Western blots with antibodies against the most essential cyclins in the mammalian cell cycle, cyclins A2, B1, and E1. The poor quality of anti-cyclins A2 and B1

confounded interpretation, and therefore, the remainder of my experiments were solely focused on cyclin E1 and its corresponding CDK, CDK2.

The data represented in Figures 6 – 7 strongly suggests that the proliferative effect of IGF-1 is not associated with cyclin E1 expression, but rather with the phosphorylation of CDK2, as cyclin E1 expression did not increase in cardiomyocytes induced with IGF-1 but phosphorylation of CDK2 increased. This finding agrees with cell cycle literature – when mammalian cells enter the cell cycle, endogenous expression of cyclins is not enhanced (Lodish, 2014; p. 884). Instead, CDKs associate with their respective cyclins and undergo phosphorylation, resulting in activation of their kinase activity (Lodish, 2014; p. 885).

As Figure 10 illustrates, CDK2 phosphorylation appears to be AKT-dependent, as treatment with triciribine decreased pCDK2 to basal levels of phosphorylation. Furthermore, the phospho-CDK2 antibody used in this study detected phosphorylation by CAK. Considering that this phosphorylation site (Thr 160) was modified by AKT inhibition suggests that CDK2 activity is controlled by AKT via the CAK complex.

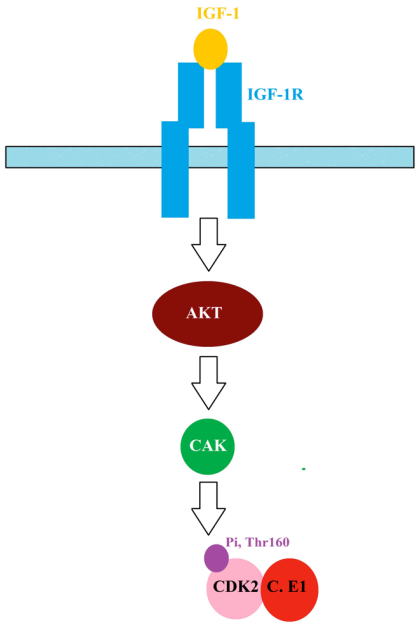


To confirm the role of the CAK complex in AKT-dependent CDK2 phosphorylation, the CAK complex in cardiomyocytes was knocked down and probed with anti-pCDK2 and anti-cyclin E1. Protein quantitation data showed that both siRNA negative control and lipofectamine strongly affected CDK2 phosphorylation and cyclin E1 expression. Considering these effects from the controls it would be difficult to assess the effect of CAK knockdown on CDK2 phosphorylation and cyclin E1 expression in cardiomyocytes induced with IGF-1. Moreover, >90% ablation of CAK may be necessary for my experiments (Sale, 2006), and to achieve this, optimization of the transfection conditions or using CRISPR to gene-edit the cardiomyocytes would be necessary.

Additional validation of IGF1-AKT-CAK-mediated CDK2 phosphorylation will require inhibiting CDK2 phosphorylation. This could be achieved by utilizing the CDK2 inhibitor Flavopiridol (Selleckchem) and performing Western blot analysis. To confirm the role of IGF1-AKT-CAK-activated CDK2 in cardiomyocyte proliferation, BrdU

proliferation assays would be performed on Flavopiridol-treated cardiomyocytes; minimal proliferative activity will be indicative of a role for CDK2.

*The use of sequencing primers, an alternate to traditional site-directed mutagenesis.*

When attempting to introduce dominant negative and constitiutievly active mutations into a CDK7 plasmid, DpnI site-directed mutagenesis was unsuccesful. This was despite altering thermocycling conditions in a number of ways, including increasing the annealing temperature to reduce non-specfic binding; increasing denaturation time to allow for a more complete denaturing of DNA and sufficient access for primers to anneal; increasing elongation time as well as increasing cycle number (Roche, 2016). To verify efficient bacterial transformation, parental plasmid DNA was diluted 1:100, transformed, and plated on an agar plate. Bacterial colonies were present the next day, suggesting that the strategy to adjust PCR conditions was the correct option. However, none of these modifications worked so an alternative two-step strategy was adopted. This involved the use of sequencing primers to sequencing sites within the plasmid, which are well-established with respect to PCR amplification. They are also useful for restriction digests as they lie far outside the cloning sites. Restriction enzymes require a certain number of base pairs on the 5'end to cut successfully (New England Biosciences, 2016). Employing sequencing primers guarentees the presence of significant stretches of DNA on either side of multiple cloning sites and thereby, successful restriction enzyme digests.

There was an issue with parental plasmid contamination, necessitating another series of PCR optimization steps – reducing cycle number from 35 to 25 to reduce amplification of

contaminants; gel purification of individual construct bands to ensure isolation of the specific DNA fragments in the absence of the contaminating parental plasmid which would run at a higher molecular weight; using equal molarities of the respective constructs for amplification as well as modifying DNA concentration to reduce non-specific amplification. These approaches were unsuccessful in preventing amplification from contaminating parental plasmid. Interestingly doubling the concentration of Mg++, in addition to the previous alterations described above, showed only a limited amount of amplification from the parental plasmid. This may be due to enhancement activity of the polymerase (Caister Academic Press, 2016). Increasing Mg++ reduces the ability of DNA to denature, thus the higher Mg++ concentration may have prevented denaturation of the larger sized plasmid whilst still allowing primer access to the much smaller DNA fragments.

The next step would be to digest the amplicon and ligate it into the empty parental plasmid, perform bacterial transformation, and further characterize kanamycin resistant colonies for the presence of the insert and faithful copying of the DNA (i.e. sequencing to ensure the correct sequence). Once the plasmid DNA is isolated cardiomyocytes would be transfected with plasmids that contain the dominant negative form of CAK or the constitutively active form of CAK. Transfection with the empty plasmid and a plasmid containing wild-type CDK7 would serve as controls. Following transfection, Western blot analysis would be performed as described above on all groups to ensure that mutations were affecting activity of CDK7 and examine how this modifies CDK phosphorylation and cyclin expression. Afterwards, BrdU proliferation assays would be

performed as a final readout. I expect to see the highest amount of proliferation in wells with cells containing the constitutively active CAK construct and the lowest amount of proliferation in wells with cells containing the dominant negative CAK construct.

**References**


Abcam. Anti-CDK1 (phospho Y15) antibody [EPR7875] (ab133463) [Internet].Cambridge (MA).Abcam [cited 2015 Nov 4]. Available from http://www.abcam.com/cdk1-phospho-y15-antibody-epr7875-ab133463.html.

Abcam. Anti-CDK2 (phospho Y15) antibody [EPR2233Y] (ab76146) [Internet].Cambridge (MA).Abcam [cited 2015 Nov 4]. Available from http://www.abcam.com/cdk2-phospho-y15-antibody-epr2233y-ab76146.html.

Abcam. Anti-RNA polymerase II CTD repeat YSPTSPS (phospho S5) antibody - ChIP Grade (ab5131). [Internet].Cambridge (MA).Abcam [cited 2015 Nov 4]. Available from http://www.abcam.com/rna-polymerase-ii-ctd-repeat-ysptsps-phospho-s5-antibody-chip-grade-ab5131.html.

Abcam. Western blot troubleshooting tips [Internet].Cambridge (MA). Abcam [cited 2015 Nov 3]. Available from http://www.abcam.com/protocols/western-blot-troubleshooting-tips.

Baksh S., Akshay Bareja, Conrad Hodgkinson, Jonah Yusif, Shubham Patel, Victor J Dzau. The Effects of Biased Ligand Signaling on Cardiomyocyte Proliferation. Poster session presented at: 11th Annual Johns Hopkins Biotechnology Research Symposium; 2016 May 10; Rockville, MD.

Anderson, Gwendolyn J., Cynthia Cipolla, Robert T. Kennedy. 2011. Western Blotting using Capillary Electrophoresis. *Anal Chem*. 83(4): 1350–1355.

Bordeaux, Jennifer, Allison W. Welsh, Seema Agarwal, Elizabeth Killiam, Maria T. Baquero, Jason A. Hanna, Valsamo K. Anagnostou, David L. Rimm. 2010. Antibody validation. *Biotechniques*. 48(3): 197–209.

Boxem, Mike. 2006. Cyclin-dependent kinases in C. elegans. *Cell Division*. 1(6). doi: 10.1186/1747-1028-1-6

Beigi, F., J Schmeckpeper, P Pow-Anpongkul, JA Payne, L Zhang, Z Zhang, J Huang, M Mirotsou, VJ Dzau. 2013. C3orf58, a novel paracrine protein, stimulates cardiomyocyte cell-cycle progression through the PI3K-AKT-CDK7 pathway. *Circ Res*. 113(4):372-80.

Bergmaan, O., RD Bhardwaj, S Bernard, S Zdunek, F Barnabé-Heider, S Walsh, J Zupicich, K Alkass, BA Buchholz, H Druid, S Jovinge, J Frisén. 2009. Evidence for cardiomyocyte renewal in humans. *Science*. 3;324(5923):98-102.

Brown University. Complications of Acute Myocardial Infarction [Internet]. Providence (RI). Brown University [cited 2015 Nov 3]. Available from http://www.brown.edu/Courses/Bio_281-cardio/cardio/handout4.htm.

Caister Academic Press – PCR Troubleshooting [Internet]. Poole, UK. Caister Academic Press [cited 23 August 2016]. Available from http://www.highveld.com/pcr/pcr-troubleshooting.html

Centers for Disease Control and Prevention. 2015. Life After a Heart Attack [Internet]. Atlanta (GA). Centers for Disease Control and Prevention; [cited 2015 Nov 1]. Available from http://www.cdc.gov/heartdisease/heart_attack_recovery.htm.

Chang, F., L S Steelman, J T Lee, J G Shelton, P M Navolanic, W L Blalock, R A Franklin, J A McCubrey. 2003. Signal transduction mediated by the Ras/Raf/MEK/ERK pathway from cytokine receptors to transcription factors: potential targeting for therapeutic intervention. *Leukemia.* 17(7):1263-93.

Garibyan, Lilit, Nidhi Avashia. 2013. Polymerase Chain Reaction. *Journal of Investigative Dermatology*. 133, e6. doi:10.1038/jid.2013.1.

Weizmann Institute of Science. CDK1 Gene [Internet]. Rehovot, Israel. Gene Cards Suite [cited 2 June 2016]. Available from http://www.genecards.org/cgi-bin/carddisp.pl?gene=CDK1

Gene Tools, LLC. Morpholino Antisense Oligos [Internet]. Philomath (OR) Gene Tools, LLC; [cited 2015 Nov 1]. Available from http://www.gene-tools.com/morpholino_antisense_oligos.

Girnita, A., H Zheng, A Grönberg, L Girnita, M Ståhle. 2012. Identification of the cathelicidin peptide LL-37 as agonist for the type I insulin-like growth factor receptor. *Oncogene.* 31(3): 352–365.

Hong, Sun Woo, Seong Min Honga, Jae Wook Yooa,b, Young Chul Leec, Soyoun Kimd, John T. Lise, Dong-ki Lee. 2009. Phosphorylation of the RNA polymerase II C-terminal domain by TFIIH kinase is not essential for transcription of Saccharomyces cerevisiae genome. *PNAS*. 106(3): 14276–14280.

Hu, Yu-Chen. *Gene Therapy for Cartilage and Bone Tissue Engineering*. Berlin Heidelberg. Springer-Verlag. 1st Edition. 2014.

Karra, Daniela, Ralf Dahm. 2010. Transfection Techniques for Neuronal Cells. The *Journal of Neuroscience.* 30(18): 6171-6177.

Kikuchi, Kazu, Kenneth D. Poss. 2012. Cardiac Regenerative Capacity and Mechanisms. *Annu Rev Cell Dev Biol*. 28: 719–741.

Lodish, Harvey, Arnold Berk, Chris A. Kaiser, Monty Kriger, Anthony Bretscher, Hidde Ploegh, Angelika Amon, Matthew P. Scott. *Molecular Cell Biology*. New York, NY. W.H. Freeman and Company. 7th Edition. 2013.

Lolli, G., LN Johnson. 2005. CAK-Cyclin-dependent Activating Kinase: a key kinase in cell cycle control and a target for drugs? *Cell Cycle*. 2005 Apr;4(4):572-7.

Medline Plus. 2015. Heart Attack [Internet]. Bethesda (MD). National Institutes of Health; U.S. National Library of Medicine; [cited 2015 Nov 1]. Available from https://www.nlm.nih.gov/medlineplus/heartattack.html.

Meyyappan, Muthupalaniappan, Howard Wong, Christopher Hull, Karl T. Riabowol. 1998. Increased Expression of Cyclin D2 during Multiple States of Growth Arrest in Primary and Established Cells. *Mol Cell Biol*. 18(6): 3163–3172.

National Heart, Lung, and Blood Institute. 2015. What is A Heart Attack? [Internet]. Bethesda (MD). National Institutes of Health; US Department of Health and Human Services; [cited 2015 Nov 1]. Available from http://www.nhlbi.nih.gov/health/health-topics/topics/heartattack.

National Institutes of Health. 2015. CCNH Cycline H [Homo sapiens (human)] [Internet]. Bethesda (MD). National Institutes of Health; US Department of Health and Human Services; [cited 2015 Nov 7]. Available from http://www.ncbi.nlm.nih.gov/gene/902.

National Institutes of Health. 2015. MNAT1, MNAT CDK-Activating Kinase Assembly Factor 1 [Homo sapiens (human)] [Internet]. Bethesda (MD). National Institutes of Health; US Department of Health and Human Services; [cited 2015 Nov 7]. Available from http://www.ncbi.nlm.nih.gov/gene/4331.

New England Biosciences. Cleavage Close to the End of DNA Fragments. [Internet]. Ipswich (MA). New England Biosciences; [cited 23 August 2016]. Available from https://www.neb.com/tools-and-resources/usage-guidelines/cleavage-close-to-the-end-of-dna-fragments

Pasumarthi KBS, Daud AI, Field LJ. Regulation of Cardiomyocyte Proliferation and Apoptosis. In: Madame Curie Bioscience Database [Internet]. Austin (TX): [cited 2015 Nov 11] Landes Bioscience; 2000. Available from: http://www.ncbi.nlm.nih.gov/books/NBK6014/

Patel, Shetal A., M. Celeste Simon. 2010. Functional Analysis of the Cdk7·Cyclin H·Mat1 Complex in Mouse Embryonic Stem Cells and Embryos. *J Biol Chem*. 14; 285(20): 15587–15598.

Roche. Working With PCR. [Internet]. Indianapolis (IN). Roche; [cited 22 August 2016]. Available from https://lifescience.roche.com/webapp/wcs/stores/servlet/PrintView?langId=-1&storeId=14501&articleId=68077

Sale, Elizabeth M., Conrad P. Hodgkinson, Neil P. Jones, and Graham J. Sale. 2006. A New Strategy for Studying Protein Kinase B and Its Three Isoforms. Role of Protein

Kinase B in Phosphorylating Glycogen Synthase Kinase-3, Tuberin, WNK1, and ATP Citrate Lyase. *Biochemistry*. 45: 213 – 223

Salic, Adrian, Timothy J. Mitchison. 2008. A chemical method for fast and sensitive detection of DNA synthesis in vivo. *Proc Natl Acad Sci USA.* 105(7):2415-20

Schambach, Axel, Daniela Zychlinski, Birgitta Ehrnstroem, Christopher Baum. 2013. Biosafety Features of Lentiviral Vectors. *Hum Gene Ther*. 24(2): 132–142.

Schiaffino, Stefano, Cristina Mammucari. 2011. Regulation of skeletal muscle growth by the IGF1-Akt/PKB pathway: insights from genetic models. *Skelet Muscle*. 1(4). doi: 10.1186/2044-5040-1-4.

Scitable. 2014. CDK [Internet]. Cambridge (MA). Nature Education; [cited 2015 Nov 3]. Available from http://www.nature.com/scitable/topicpage/cdk-14046166.

Selleckchem. Flavopiridol (Alvocidib). [Internet]. Boston (MA). Selleckchem; [cited 23 August 2016]. Available from http://www.selleckchem.com/aboutus.html

Snyder, Mandy, Wanda Taylor. Insulin-Like Growth Factor [Internet]. Rochestesr (NY). University of Rochester Medical Center; [cited 2016 March 29]. Available from https://www.urmc.rochester.edu/encyclopedia/content.aspx%3FContentTypeID%3D167%26ContentID%3Dinsulin_like_growth_factor

Suryadinata, Randy, Martin Sadowski, Boris Sarcevic. 2010. Control of cell cycle progression by phosphorylation of cyclin-dependent kinase (CDK) substrates. *Bioscience Reports*. 30(4). doi:10.1042/BSR20090171

University of Maryland. 2002. TFIIH. Baltimore (MD). University of Maryland; [cited 2015 Nov 1]. Available from http://www.biochem.umd.edu/biochem/kahn/molmachines/newpolII/TFIIH.html.

Xu, Xue-Ming, Min-Hyuk Yoo, Bradley A. Carlson, Vadim N. Gladyshev, Dolph L. Hatfield. 2009. Simultaneous knockdown of the expression of two genes using multiple shRNAs and subsequent knock-in of their expression. Nat Protoc. 2009; 4(9): 1338–1348.

Zigovia, Tanja, Evan Y. Snyder, Paul R. Sanberg. *Neural Stem Cells for Brain and Spinal Cord Repair*. New York, NY. Springer Science+Business Media, LLC. 1st Edition. 2003.

# Syeda Samara Baksh

12912 MacNeil Court, Fredericksburg, VA 22407
540.479.0472 ● samarabaksh90@gmail.com


## PROFILE

Lab professional with progressive experience excelling in all levels of lab-related work within various team-oriented environments.

## EDUCATION

Sept. 2013 – Dec. 2016 Johns Hopkins University, Baltimore, MD
**Master of Science in Biotechnology**

Sept. 2008 – May 2012 University of Mary Washington, Fredericksburg, VA
**Bachelor of Science in Biology**

## RESEARCH EXPERIENCE

Jan. 2016 – Aug. 2016 **Master's Independent Research Project/Thesis, Full-time 60 – 70h/week**
"The Effect of Biased Ligand Signaling on Cardiomyocyte Proliferation"
Duke University School of Medicine, Division of Cardiology.

- Designed an original research project via extensive literature searches – an investigation of the role of IGF-1 on cardiomyocyte cell cycle reentry to promote myocardial repair – including a complete experimental protocol with minimal supervision.
- Gained proficiency in molecular biology techniques.
- Acquired experience troubleshooting experimental procedures to increase assay efficiency.
- Developed superior writing abilities through research proposal and thesis composition.
- Significantly enhanced comprehension and critical analysis of scientific literature via bimonthly journal club presentations.

Feb. 2013 – Nov. 2014 **Research Technologist, Full-time 40h/week**
Johns Hopkins University School of Medicine, Bayview Medical Center, Division of Pulmonary and Critical Care

- Learned and performed a range of experimental techniques, such as Western blotting and intracellular calcium imaging.
- Acquired experience delivering presentations and lectures to lab members.
- Routinely trained and advised laboratory personnel.
- Managed policies, personnel, and finances in a molecular biology laboratory; ensured compliance with applicable standards and coordinated maintenance and repairs of equipment.

Sept. 2010 – May 2012 **Undergraduate Research Assistant, Part-time 4 – 5h/week**
"Cell Fusion and Growth Factor IGF in Myocardial Repair"
University of Mary Washington, Biology Department

- Designed an original research project– an investigation of the role of IGF in cardiomyocyte and cardiac stem cell fusion to promote myocardial repair – with close supervision.

- Maintained communication with research advisor while working independently in order to acquire and interpret results.
- Delivered accurate and detailed scientific records.

## RELEVANT COURSEWORK AND LABORATORY SKILLS

Immunology
- Enzyme-linked Immunosorbent Assay
- Polyacrylamide Gel Electrophoresis
- Hemagglutination Assay
- Western Blotting
- Affinity Column Purification
- BrdU Proliferation Assay
- Immunofluorescent Staining

Molecular Biology
- Small Animal Surgery
- Tissue Culture
- Cell Isolation
- Cell Passaging
- Fluorescent Microcopy
- Cryopreservation
- Intracellular Calcium Imaging
- BCA Protein Assay
- siRNA Transfection
- PCR Site-Directed Mutagenesis
- DNA/RNA Purification and Quantitation
- Recombinant Plasmid Production
- DpnI Cloning

Genetics
- Reverse Transcription and Real Time Quantitative Polymerase Chain Reaction
- Drosophila Genotyping and Phenotyping
- Electrophoresis-based Genotyping

Microbiology
- Gram Staining
- Aseptic Technique
- Serial Dilutions
- Bacterial Transformation

Virology
- Plaque Assay
- $TCID_{50}$ Assay
- Viral Transduction

Statistics
- Data Analysis
- Data Production
- Probability
- Statistical Inference

## PRESENTATIONS AND PUBLICATIONS

### PUBLICATIONS

1) **Baksh, S**. "The Effect of Biased Ligand Signaling on Cardiomyocyte Proliferation." (Master's thesis: defended Aug 2016). Johns Hopkins University, 2017. Available in JScholarship.

2) Suresh K, Servinsky L, Reyes J, **Baksh S**, Undem C, Caterina M, Pearse DB, Shimoda LA. "Hydrogen peroxide-induced calcium influx in lung microvascular endothelial cells involves TRPV4." *American Journal of of Physiology – Lung Cellular and Molecular Physiology.* 2015 Dec 15; 309(12):1467-77.

3) Lai N, Lade J, Leggett K, Yun X, **Baksh S,** Chau E, Crow MT, Sidhaye V, Wang J, Shimoda LA. "The aquaporin 1 C-terminal tail is required for migration and growth of pulmonary arterial myocytes." *American Journal of Respiratory Medicine*. 2014 Jun; 50(6):1010-20

4) **Baksh S**, Loesser K. "Cell Fusion and Growth Factor IGF in Myocardial Repair." Abstract and oral presentation delivered at the Virginia Academy of Science, Norfolk, VA. 2012

## GRANTS

1) Moon K, **Baksh S**, Punjabi N, Shimoda LA. "Calcium Signaling and Glucose Output In Hepatocytes After In Vivo Exposure To Intermittent Hypoxia." American Thoracic Society, 2014.

## POSTERS

1) **Baksh S,** Hodgkinson C, Bareja A, Yusif J, Patel S, Dzau VJ. "Effects of Biased Ligand Signaling on Cardiomyocyte Proliferation." Johns Hopkins Biotechnology Research Symposium 2016.

2) Maman S, **Baksh S**, Yun X, Jiang H, Shimoda LA. "Mechanisms Involved in Hypoxia-Inducible Factor 1 Dependent Upregulation of Aquaporin 1." Hopkins C.A.R.E.S Summer Symposium 2014.

3) Maman S, **Baksh S**, Yun X, Jiang H, Shimoda LA. "The Role of Hypoxia-Inducible Factor 1 in Upregulation of Aquaporin 1 Channels in Pulmonary Arterial Smooth Muscle Cells." John's Hopkins Summer Internship Program Poster Presentation 2013.

## ADDITIONAL SKILLS

Computer Skills – Microsoft Word 2016, Excel 2016, and PowerPoint 2016

Languages – Fluent in Bengali